Advanced Composite Materials
Publication details, including instructions for authors and subscription information:
http://www.tandfonline.com/loi/tacm20

Electrical Resistance Change under Strain of CNF/Flexible-Epoxy Composite

Tetsuo Yasuoka [a] , Yoshinobu Shimamura [b] & Akira Todoroki [c]

[a] Tonen General Sekiyu K.K., Kawasaki Refinery, 7-1 Ukishima-cho, Kawasaki-ku, Kawasaki, Kanagawa 210-8523, Japan

[b] Shizuoka University, Department of Mechanical Engineering, 3-5-1 Johoku, Naka-ku, Hamamatsu, Shizuoka 432-8561, Japan;, Email: tysimam@ipc.shizuoka.ac.jp

[c] Tokyo Institute of Technology, Department of Mechanical Sciences and Engineering, 2-12-1 O-okayama, Meguro-ku, Tokyo 152-8552, Japan

Version of record first published: 02 Apr 2012.

VSP

Advanced Composite Materials 19 (2010) 123–138

ADVANCED COMPOSITE MATERIALS
brill.nl/acm

Electrical Resistance Change under Strain of CNF/Flexible-Epoxy Composite

Tetsuo Yasuoka [a], **Yoshinobu Shimamura** [b,*] **and Akira Todoroki** [c]

[a] Tonen General Sekiyu K.K., Kawasaki Refinery, 7-1 Ukishima-cho, Kawasaki-ku, Kawasaki, Kanagawa 210-8523, Japan

[b] Shizuoka University, Department of Mechanical Engineering, 3-5-1 Johoku, Naka-ku, Hamamatsu, Shizuoka 432-8561, Japan

[c] Tokyo Institute of Technology, Department of Mechanical Sciences and Engineering, 2-12-1 O-okayama, Meguro-ku, Tokyo 152-8552, Japan

Received 23 March 2009; accepted 2 April 2009

Abstract

Carbon nanofibers (CNFs) have good electrical conductivity. Addition of a few percent of carbon nanofibers to polymers yields electrical conductivity but hardly affects the mechanical properties of the polymers. These conductive polymers may be useful for sensing applications, such as strain sensors and chem-resist sensors. Many researchers have reported on the electrical conductivity, but the electrical resistance change under strain, i.e. piezoresistivity, of the carbon nanofiber filled resin has not been fully investigated. In this study, the electrical resistance change under strain of CNF/flexible-epoxy composites was investigated experimentally and analytically. Experimental results show that the electrical resistance change under strain is non-linear and much larger than that in metal, and the sensitivity of the electrical resistance change to strain decreases as the weight fraction of CNF increases. The mechanism of the electrical resistance change under strain of CNF/polymer composites was discussed by using electrical circuit simulation based on a percolation network model and tunneling effect between CNFs. The results imply that the non-linear behavior is caused by tunneling resistance change between CNFs, and that the decrease of sensitivity with increasing weight fraction of CNF is caused by the nature of the percolation network.

Keywords

Carbon nanofiber, nanocomposite, piezoresistivity, percolation, tunneling effect

1. Introduction

Carbon nanofibers (CNFs), including carbon nanotubes, are tubular materials which consist only of carbon atoms. The order of diameter is nanometers. CNFs have high aspect ratio and excellent mechanical, thermal and electrical properties. Thus,

* To whom correspondence should be addressed. E-mail: tysimam@ipc.shizuoka.ac.jp
Edited by the JSCM

DOI:10.1163/092430410X490446

CNFs are good candidates as filler for resin. Many researchers have reported that the addition of CNFs into resin enhances electrical conductivity of the resin [1–14]. For example, applications to electro-magnetic interference sealed materials [1] and piezoresistive sensors [2, 3] are proposed.

The weight fraction of CNF to yield electrical conductivity is much lower than that of carbon black [14], which is the typical conductive filler for resin. Using CNF as filler can, therefore, give electrical conductivity with less degradation of mechanical properties of the resin, such as elasticity and elongation. Our idea is to use CNF-filled elastomer for large strain measurement more than 10%. For the purpose, the electrical resistance change under strain, i.e. piezoresistivity, should be investigated. Several experimental researches on piezoresistivity of CNF-filled non-elastomeric [15–21] and elastomeric resins [22, 23] have been reported and several theoretical approaches to explain the piezoresistivity have been reported [20, 24]. The behavior and mechanism of piezoresistivity of CNF-filled elastomeric resin is, however, not clear.

In this study, CNF-filled elastomers were fabricated and electrical resistance changes under strain for various weight fractions were measured. The experimental results show that the piezoresistivity of CNF-filled elastomers is non-linear and has high sensitivity as compared with metal, and that the increase of the weight fraction of CNF decreases the sensitivity. Then, a circuit model based on percolation network and tunneling effect was proposed. The piezoresistivity was simulated by using the circuit model. The simulation results reveal that tunneling resistance change mainly contributes to the non-linear electrical resistance change.

2. Electrical Resistance Change under Strain

2.1. Materials

Several types of carbon nanofibers are available in the commercial market. A typical one is carbon nanotube [25], whose diameter ranges from a few nm to tens of nm. Carbon nanotubes are, however, expensive for use as fillers and it is difficult to disperse them into resin because carbon nanotubes have high aspect ratio and specific surface ratio. In this study, vapor grown carbon fiber (VGCF, graphitized) [26] supplied by Showa Denko K. K. was used as electrical conductive filler. The difference between VGCF and CNT is the diameter. The average diameter of VGCF is 150 nm, which is much thicker than that of CNT. Table 1 shows the dimensions and material properties of VGCF and Fig. 1 shows a SEM picture of VGCF.

Two types of flexible-epoxy are used as elastomeric matrix. The first one is Epikote 871/Epomate LX1N by Japan Epoxy Resins Co. Ltd., which has 30% of elongation, and the other one is ME-113/XH-1859-2 by Nippon Pelnox Corporation, which has 150% of elongation. Hereafter, we designate Epikote 871/Epomate LX1N as Epoxy A, and ME-113/XH-1859-2 as Epoxy B.

Table 1.
Dimensions and properties of VGCF

Diameter	150 (nm)
Length	10–20 (μm)
Aspect ratio	10–500
Density	2.0 (g/cm^3)
Resistivity	1×10^{-4} (Ωcm)

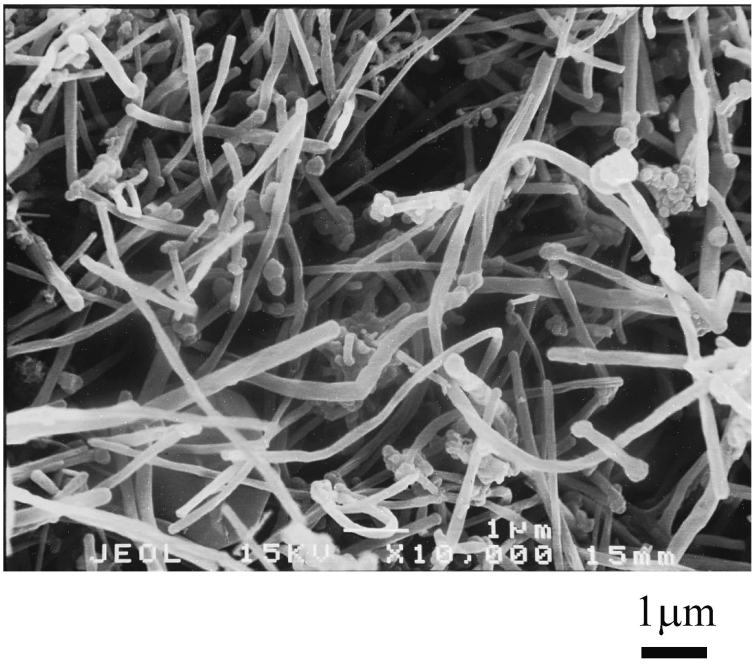

Figure 1. SEM picture of VGCF.

2.2. *Specimen*

The specimen configuration for electrical resistance change measurement under strain is shown in Fig. 2. A VGCF/flexible-epoxy composite layer is sandwiched between two aluminum blocks used for grips and electrodes. VGCF of 1.0 wt%, 1.5 wt%, 2.0 wt%, 2.5 wt% or 3.0 wt% was added into Epoxy A, and VGCF of 2.0 wt%, 2.5 wt% or 3.0 wt% was added into Epoxy B. For Epoxy B, electrical conductivity did not appear in the case of 1.0 wt% or 1.5 wt%.

VGCF was dried in a furnace at 130°C for 2 h, and epoxy, hardener and VGCF were mixed by using a planetary mixer (NBK-1, NISSEI Corporation) for 10 min with 2000 rpm. The mixture was poured into a mold and co-cured with the aluminum blocks. Epoxy A and Epoxy B were cured at 80°C for 3 h and at 85°C for 7 h, respectively.

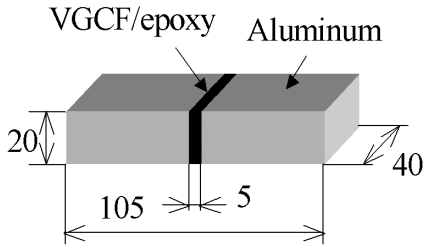

Figure 2. Specimen configuration.

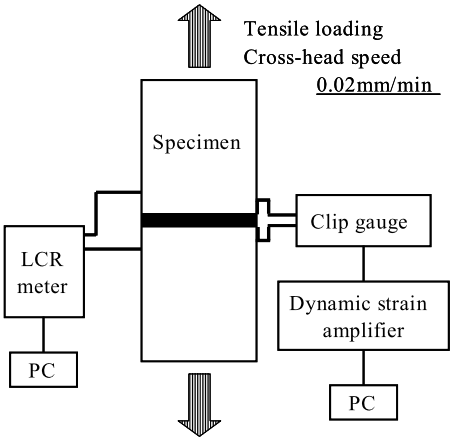

Figure 3. Experimental method and measurements.

2.3. Electrical Resistance Change under Strain

Figure 3 shows an experimental method to measure electrical resistance change under strain. Tensile tests were conducted by using a tensile testing machine (AG-I 100 kN, Shimadzu Corporation). The cross-head speed was 0.02 mm/min. Three specimens were prepared for Epoxy A with 1.0 wt% and 1.5 wt% of VGCF and one specimen was prepared for Epoxy A with 2.0, 2.5 and 3.0 wt% of VGCF. Two specimens were prepared for Epoxy B with each weight fraction of VGCF. During tensile tests, elongation of the composite part was measured by using a clip gauge and DC electrical resistance was measured by using an LCR meter (3522, HIOKI). The electrical resistance of the composite part was so high that it is possible to use a two-electrode method for measuring the electrical resistance.

2.4. Results

At first, dispersion of VGCF in resin was observed by using a SEM (JSM-6301, Jeol Ltd.). A typical SEM image of the surface of VGCF filled composites is shown in Fig. 4. Good dispersion of VGCF in resin was confirmed.

Volume resistivities of composites are shown in Fig. 5. The vertical axis is the volume resistivity and the horizontal axis is the weight fraction of VGCF. The re-

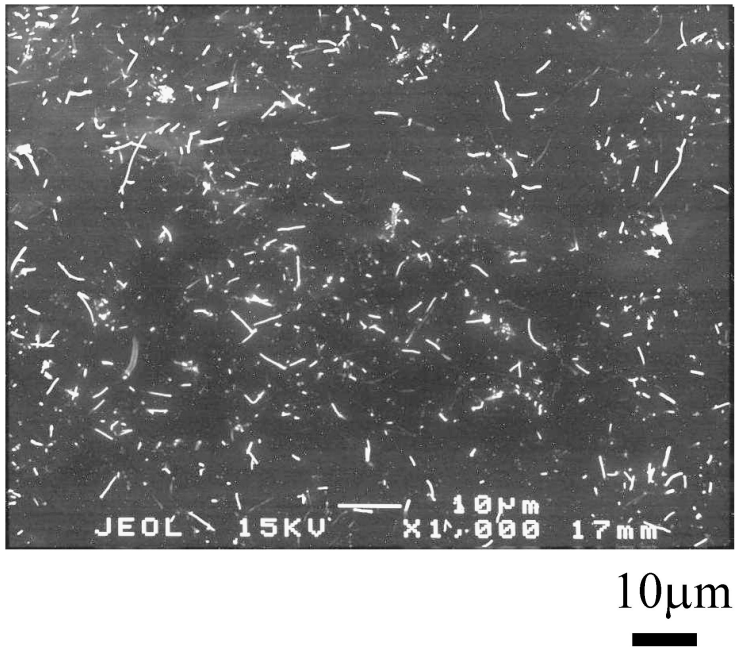

Figure 4. SEM observation of VGCF dispersion (3.0 wt%).

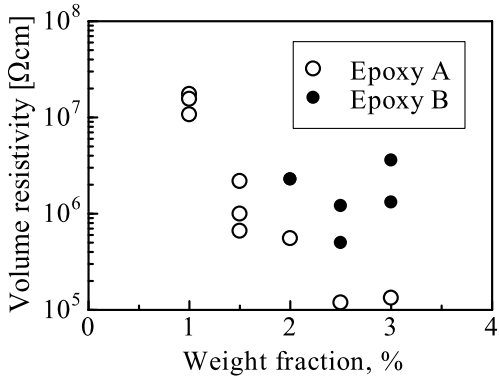

Figure 5. Volume resistivity of specimen.

sults show that the addition of CNF results in the decrease of volume resistivity but the scatter band is wide. For Epoxy B, electrical conductivity did not appear when the weight fraction was 1.0 wt% or 2.0 wt%. The difference between electrical resistivities of two epoxy systems seems to result from the difference of viscosity between two epoxy systems, which may affect the degree of dispersion of VGCF during mixture.

Electrical resistance changes under strain for Epoxy A and Epoxy B are shown in Figs 6 and 7, respectively. The vertical axis is the electrical resistance change

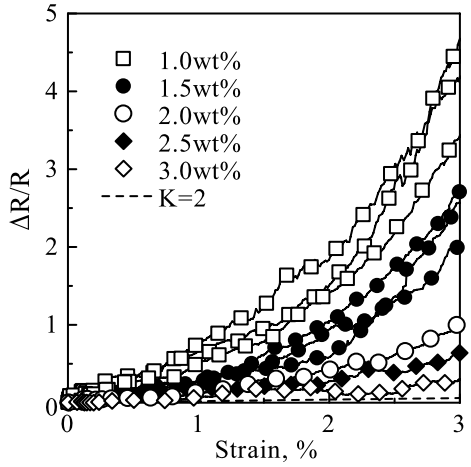

Figure 6. Electrical resistance change (Epoxy A).

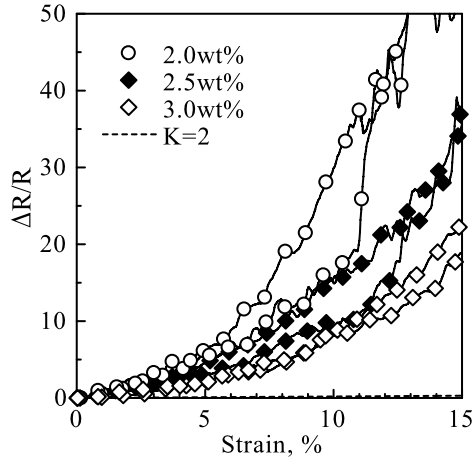

Figure 7. Electrical resistance change (Epoxy B).

and the horizontal axis is the applied strain. The results are shown only when the stress–strain relationships are linear. In both figures, the electrical resistance change of general metals (gauge factor $K = 2$) is shown by a broken line for reference.

The electrical resistance changes of composites are significantly non-linear while metals and semiconductors used for conventional strain gauges have linear relations. The sensitivity of electrical resistance changes to strain, which corresponds to gauge factor, are much higher than that of strain gauge made from metals and are compared with that of strain gauge made from semiconductors. The increase of VGCF weight fraction decreases the sensitivity. The electrical resistance changes under strain up to $\varepsilon = 3\%$ for Epoxy B are almost similar to those for Epoxy A. So the matrix seems to less affect the electrical resistance change.

3. Mechanism of Electrical Resistance Change

The behavior of electrical resistance change under strain of VGCF filled flexible-epoxy is different from that of metals and semiconductors. Taya *et al*. [24] explained piezoresistivity of short fiber reinforced elastomers in terms of percolation network with the orientation change of short fibers and the distance change between short fibers. Hu *et al*. [21] explained piezoresistivity of carbon nanotube filled resin composites in terms of tunneling resistance between cabon nanotubes.

In this study, we propose a circuit model including both percolation network and tunneling effect in order to discuss the mechanism of piezoresistivity. The electrical resistance change under strain is simulated by using the circuit model and compared with the experimental results.

3.1. Conductive Network and Contact Resistance

In order to model the conductive network of VGCF in flexible-epoxy resin, we assume:

- Formation of conductive network obeys the percolation theory [27–31].
- Contact resistance between VGCFs is equal to the tunneling resistance between VGCFs [32].
- The resistance of VGCF itself is much lower than the contact resistance.

Many researchers have proved that formation of a conductive network of carbon nanofibers obeys the percolation theory [5–14]. For example, Fig. 5 shows rapid decrease of volume resistance with increase in the weight fraction of VGCF. According to the percolation theory, the relationship between the volume resistance and the volume fraction can be described as

$$\rho = \rho_0 (V_\mathrm{f} - V_\mathrm{f}^*)^{-t}, \tag{1}$$

where ρ is the volume resistivity, ρ_0 is a scale factor, V_f is the volume fraction, V_f^* is the threshold of the volume fraction and t is a critical exponent.

In this study, it is assumed that the contact resistance between carbon nanofibers is equal to the tunneling resistance between carbon nanofibers. If perfect plane contact between graphene sheets is achieved, the contact resistance seems to be negligible. However, carbon nanofibers have curvature. Carbon nanofibers make point contacts and thus, tunneling conduction occurs around the point contact region. The electrical resistance at the tunneling conduction is called tunneling resistance. The relationship between applied strain and tunneling resistance is derived as follows.

When the voltage between carbon nanofibers is small, the electrical current density J between carbon nanofibers is described as [33]

$$J = \frac{e^2\sqrt{2m\varphi}}{h^2 s} V \exp\left(-\frac{4\pi s\sqrt{2m\varphi}}{h}\right), \tag{2}$$

where e is an elementary charge, m is the mass of an electron, h is Plank's constant, ϕ is the potential height from Fermi level η, s is the distance between conductors,

i.e. tunneling distance, and V is the voltage between two conductors. In this study, the tunneling region is assumed to be a vacuum because fiber contact is discussed. Tunneling resistance r is derived from equation (2).

$$r = \frac{V}{AJ} = \frac{h^2 s}{Ae^2\sqrt{2m\varphi}} \exp\left(\frac{4\pi s\sqrt{2m\varphi}}{h}\right), \tag{3}$$

where A is the conduction area.

The distance change between conductors, i.e. carbon fibers, is calculated from geometrical change under strain [24]. Figure 8 shows a schematic illustration of the contact area. In this study, plane strain condition is assumed. Applied strain changes the distance between carbon nanofibers from s_0 to s_1 and the conduction area from A_0 to A_1. s_1 is described as

$$s_1 = s_0(1 + \varepsilon_1 \cos^2\theta + \varepsilon_2 \sin^2\theta), \tag{4}$$

where ε_1 and ε_2 are the strains in the y direction and in the x direction, respectively, and θ is the angle of the conductive path from the y direction.

The electrical resistance change ratio r_1/r_0 is calculated from equation (3).

$$\frac{r_1}{r_0} = \frac{s_1}{s_0}\frac{A_0}{A_1} \exp\left(\frac{4\pi\sqrt{2m\varphi}}{h}(s_1 - s_0)\right). \tag{5}$$

Substituting equation (4) into equation (5), we can obtain

$$\frac{r_1}{r_0} = (1 + \varepsilon_1 \cos^2\theta + \varepsilon_2 \sin^2\theta)\frac{A_0}{A_1} \exp\left(\frac{4\pi\sqrt{2m\varphi}}{h} s_0(\varepsilon_1 \cos^2\theta + \varepsilon_2 \sin^2\theta)\right). \tag{6}$$

Equation (6) gives the change in tunneling resistance under strain. Since the tunneling resistance change is an exponential function of applied strain, the total electrical resistance change of bulk composite is supposed to increase exponentially due to applied strain.

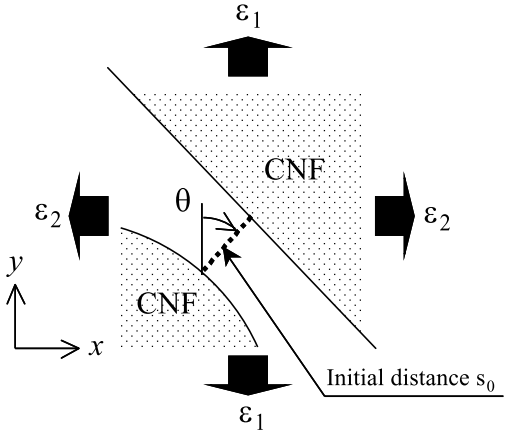

Figure 8. Distance change between CNFs.

The third assumption is appropriate because the volume electrical resistance of VGCF, which is 1.0×10^{-4} Ωcm, is much smaller than the contact resistance calculated from equation (3).

3.2. Simulation of Piezoresistivity by Using Circuit Model

In order to discuss the mechanism of piezoresistivity, electrical circuit simulation was carried out by using a SPICE circuit simulator. A circuit model for simulation is shown in Fig. 9. In this study, a two-dimensional model is used for simplicity. CNFs are reticulated to form a percolation network. In Fig. 9, a node represents a CNF, and a resistance component represents a contact resistance between CNFs. The contact resistance is calculated according to equation (3). Each CNF has four diagonal contact points because a diagonal contact can represent a longitudinal, transverse or oblique contact, which appears in actual composites. Though a reticulated network is adopted in this simulation, the contact angle in equation (6) ranges randomly from 0° to 180°. In this model, a CNF is represented as a point so the effects of the shape and size of CNF are not included in this simulation.

The volume fraction of CNF corresponds to the number of contact resistance, i.e. the ratio p of contact resistance to the maximum number of contacts N_T, because an increase of contact points means the increase of the volume fraction of CNF. In order to simulate the random distribution of CNFs in the matrix, resistance elements are randomly placed in the network configuration. An example for $N_T = 50$ is shown in Fig. 10. In the case of $p = 0\%$, no resistance element exists and, thus, no conductive path is formed. In the case of $p = 60\%$, conductive paths are partially formed. In the case of $p = 100\%$, conductive paths are perfectly formed.

For preparatory simulation, the electrical resistances of the model were calculated for various ratios p without applied strain by using the parameters listed in

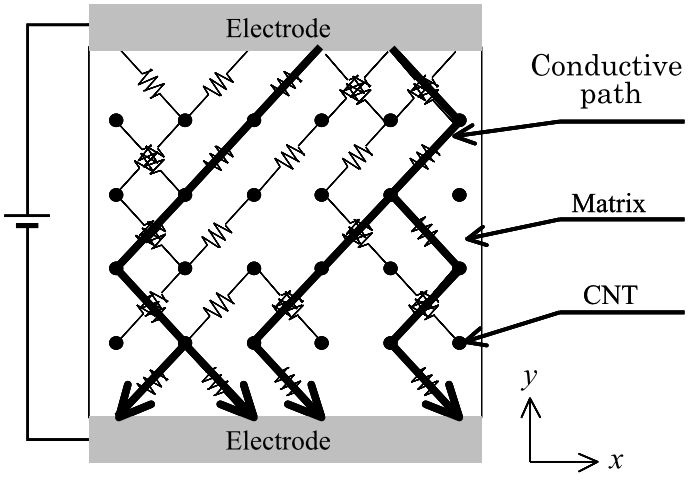

Figure 9. Analytical circuit model.

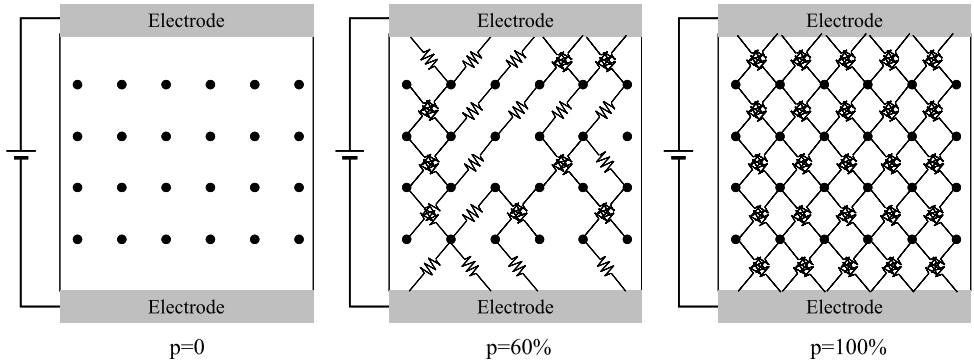

Figure 10. Probability of tunneling resistance existence.

Table 2.
Parameters for simulation

Plank's constant	$h = 6.6261 \times 10^{-34}$ (Js)
Elementary charge	$e = 1.6022 \times 10^{-19}$ (C)
Mass of electron	$m = 9.109 \times 10^{-31}$ (kg)
Distance between CNFs	0.34 (nm) $< s_0 <$ 1 (nm) (random value)
Area of conduction	$A = (150\ (\text{nm}))^2$
Barrier height*	$\Phi = 4.3$ (eV)
Poisson's ratio	$v = 0$
Angle of CNF gap	$0 < \theta < \pi$ (random value)
The maximum number of resistance N_T	80 000

*Barrier height is assumed to be the work function of vacuum [34].

Table 2. The tunneling distance is randomly set to from 0.34 nm to 1 nm: 0.34 nm is the interlayer distance of multiwall carbon nanotubes, and 1 nm is the upper limit of tunneling conduction in general. The maximum number of resistance N_T is 80 000, and this is sufficient to produce convergence of the results. The results are shown in Fig. 11. The vertical axis is the electrical resistance normalized by that with $p = 100\%$, and the horizontal axis is the ratio p of contact resistance. In Fig. 11, open circles represent the simulated results, and a solid line represents an approximation by using equation (1) where V_f is replaced by p. The approximation agrees well with the simulated results. In other words, this model can simulate the percolation phenomenon of electrical conduction. The percolation threshold $p = 54.8\%$ in the simulation corresponds to the experimental threshold volume fraction of VGCF. Similarly, the electrical resistance at $p = 100\%$ is so low that $p = 100\%$ corresponds to more than 3 wt%. Since the weight fraction of VGCF in this study is between the threshold and 3 wt%, the proposed model can simulate our composite system.

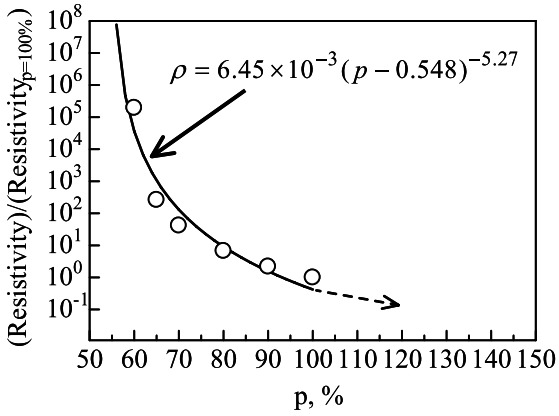

Figure 11. Electrical resistance change by simulation.

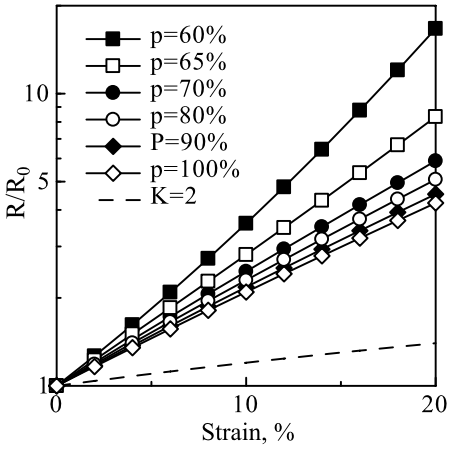

Figure 12. Analytical electrical resistance change.

3.3. Electrical Resistance Change under Strain

Analytical procedures are as follows: resistance elements are randomly placed to form a circuit; the electrical resistance of each resistance element without applied strain is determined by using equation (3) and Table 2; the total resistance of the circuit is calculated by using a SPICE simulator; the distance s_1 between carbon nanofibers in each resistance element under applied strain is calculated by using equation (4) and the electrical resistance of each element is recalculated by using equation (3); and the total resistance of the circuit under applied strain is then recalculated by using the SPICE simulator. The applied strain is changed from 0% to 20% at an interval of 2%. Simulations were conducted at $p = 60\%$, 65%, 70%, 80%, 90% and 100%.

The results are shown in Fig. 12. The vertical axis is the electrical resistance normalized by that without applied strain with log scale, and the horizontal axis is the

applied strain. Since the electrical resistance is linear in Fig. 12, the electrical resistance change is exponentially proportional to the applied strain. Remember that the tunneling resistance is exponentially proportional to the applied strain as described in equation (6). In addition, the gauge factor decreases with increasing the ratio p of resistance elements. Experimental results are replotted in Figs 13 and 14 with the same vertical axis of Fig. 12. Experimental results are also linear in Figs 13 and 14. The order of the electrical resistance change in experiments is comparable to that in the analyses. The dependency of gauge factor on volume fraction of VGCF appears in simulation.

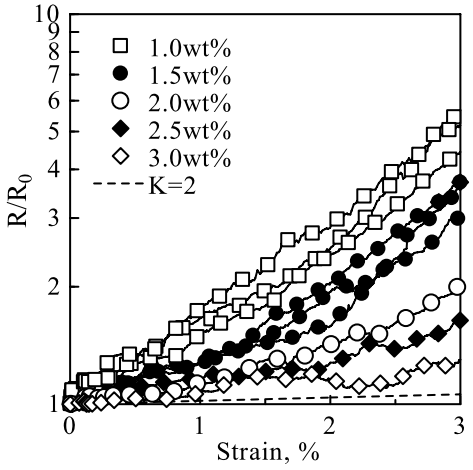

Figure 13. Electrical resistance change (Epoxy A, Log scale).

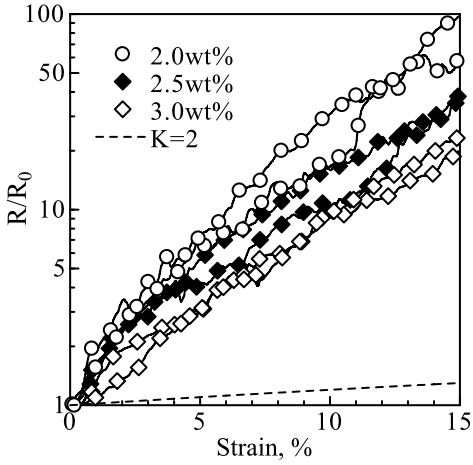

Figure 14. Electrical resistance change (Epoxy B, Log scale).

It is worth noting that the exponential change is not disadvantageous to make practical strain sensors because linear output can be obtained by using a log amplifier.

3.4. Discussions

In the previous section, the piezoresistivity of VGCF/epoxy composites is well simulated by incorporating a percolation network and a tunneling effect into a circuit model. In order to understand the contribution of tunneling resistance change and conductive network morphology change under applied strain, electrical current flows of the circuit model are visualized at $p = 60\%$ in Fig. 15 and at $p = 70\%$ in Fig. 16. Applied strain was 0%, 20% and 100%.

The difference between conductive network morphologies at $\varepsilon = 0\%$ and $\varepsilon = 20\%$ is small for both $p = 60\%$ and $p = 70\%$. This implies that the non-linear electrical resistance change under strain up to 20% mainly results from the non-linear tunneling resistance change. Conductive network morphologies at $\varepsilon = 100\%$ differs from those at $\varepsilon = 0$ and 20%. Large applied strain partly cuts off the contacts between CNFs and, thus, results in the change of the conductive network morphology. This morphology change also affects the electrical resistance of composites.

The density of the conductive network varies with the ratio p. The network density at $p = 70\%$ is evidently higher than that at $p = 60\%$. Therefore, a conductive

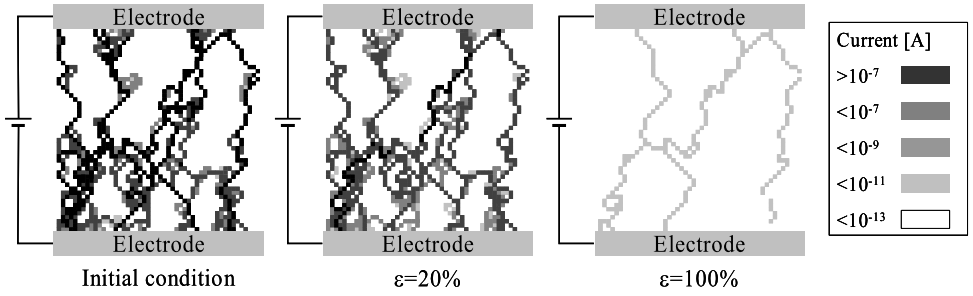

Figure 15. Change of electrical current at $p = 60\%$.

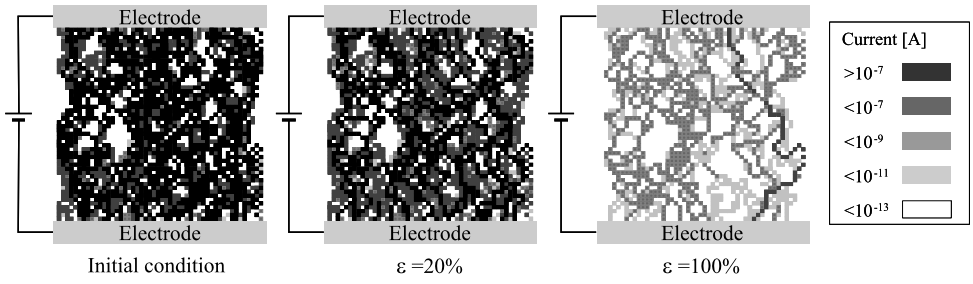

Figure 16. Change of electrical current at $p = 70\%$.

network with higher density has more capability of current detour when applied strain cuts off the network in part. This means that the sensitivity of electrical resistance to applied strain decreases with increase in the weight fraction of CNF.

The discussion revealed that the piezoresistivity behavior is caused by tunneling resistance change between CNFs and conductive network morphology change; however, the tunneling resistance change mainly contributes to the non-linear piezoresistivity behavior of the sensor under small strains.

4. Conclusions

The piezoresistivity of VGCF/flexible-epoxy was measured. The experimental results showed significant non-linearity of piezoresistivity and dependence of the gauge factor on VGCF contents. The electrical resistance change under applied strain was simulated by using a circuit simulator. It is shown that the non-linear piezoresistivity is mainly caused by tunneling resistance change between CNFs.

Acknowledgements

This work was supported, in part, by the grant from The Ogasawara Foundation for the Promotion of Science and Engineering. The authors would also like to thank Syowa Denko K. K. for VGCF supply.

References

1. M. Katsumata, H. Yamanashi, H. Ushijima and M. Endo, Electrical resistance of electroconductive plastic composite with carbon fiber filler, *Elect. Engng Japan* **114**, 17–23 (1994).
2. M. Katsumata, M. Endo and H. Ushijima, Epoxy composites using vapor-grown carbon fiber fillers for advanced electroconductive adhesive agents, *J. Mater. Res*. **9**, 841–843 (1994).
3. J. K. Abraham, B. Philip, A. Witchurch, V. K. Varadan and C. C. Reddy, A compact wireless gas sensor using a carbon nanotube/PMMA thin film chemiresistor, *Smart Mater. Struct.* **13**, 1045–1049 (2004).
4. H. Yoon, J. Xie, J. K. Abraham, V. K. Varadan and P. B. Ruffin, Passive wireless sensors using electrical transition of carbon nanotube junctions in polymer matrix, *Smart Mater. Struct*. **15**, S14–S20 (2006).
5. J. Sandler, M. S. P. Shaffer, T. Prasse, W. Bauhofer, K. Schulte and A. H. Windle, Development of a dispersion process for carbon nanotubes in an epoxy matrix and the resulting electrical properties, *Polymer* **40**, 5967–5971 (1999).
6. J. M. Benoit, B. Corraze, S. Lefrant, W. J. Blau, P. Bernier and O. Chauvet, Transport properties of PMMA-carbon nanotubes composites, *Synth. Methods* **121**, 1215–1216 (2001).
7. B. E. Kilbride, J. N. Coleman, J. Fraysse, P. Fournet, M. Cadek, A. Drury, S. Hultzler, S. Roth and W. J. Blau, Experimental observation of scaling laws for alternating current and direct current conductivity in polymer–carbon nanotube composite thin films, *J. Appl. Phys*. **92**, 4024–4030 (2002).
8. S. Barrau, P. Demont, A. Peigney, C. Laurent and C. Lacabanne, DC and AC conductivity of carbon nanotubes–polyepoxy composites, *Macromolecules* **36**, 5187–5194 (2003).

9. S. Rul, F. Lefevre-Schlick, E. Capria, C. Laurent and A. Peigney, Percolation of single-walled carbon nanotubes in ceramic matrix nanocomposites, *Acta Mater*. **52**, 1061–1067 (2004).
10. F. Du, J. E. Fischer and K. I. Winey, Effect of nanotube alignment on percolation conductivity in carbon nanotube/polymer composites, *Phys. Rev. B* **72**, 121404 (2005).
11. S. A. Gordeyev, F. J. Macedo, J. A. Ferreira, F. W. J. van Hattum and C. A. Bernardo, Transport properties of polymer–vapour grown carbon fibre composites, *Physica B* **279**, 33–36 (2000).
12. I. C. Finegan and G. G. Tibbetts, Electrical conductivity of vapor-grown carbon fiber/thermoplastic composites, *J. Mater. Res*. **16**, 1668–1674 (2001).
13. S. H. Wu, N. Toshiaki, K. Kurashiki, Q. Q. Ni, M. Iwamoto and Y. Fujii, Conductivity stability of carbon nanofiber/unsaturated polyester nanocomposites, *Adv. Compos. Mater*. **16**, 195–206 (2007).
14. K. Enomoto, T. Yasuhara, N. Ohtake and K. Kato, Injection molding of polystyrene matrix composites filled with vapor grown carbon fiber, *JSME Intl. J., Series A* **46**, 353–358 (2003).
15. J. M. Park, D. S. Kim, J. R. Lee and T. W. Kim, Nondestructive damage sensitivity and reinforcing effect of carbon nanotube/epoxy composites using electro-micromechanical technique, *Mater. Sci. Engng C* **23**, 971–975 (2003).
16. W. Zhang, J. Suhr and N. Koratkar, Carbon nanotube/polycarbonate composites as multifunctional strain sensors, *J. Nanosci. Nanotechnol*. **6**, 960–964 (2006).
17. M. Park, H. Kim and J. P. Youngblood, Strain-dependent electrical resistance of multi-walled carbon nanotube/polymer composite films, *Nanotechnology* **19**, 055705 (2008).
18. I. Kang, M. J. Shulz, J. H. Kim, V. Shanov and D. Shi, A carbon nanotube strain sensor for structural health monitoring, *Smart Mater. Struct*. **15**, 737–748 (2006).
19. G. T. Pham, Y.-B. Park, Z. Liang, C. Zhang and B. Wang, Processing and modeling of conductive thermoplastic/carbon nanotube films for strain sensing, *Composites B* **39**, 209–216 (2008).
20. M. H. G. Wichmann, S. T. Buschhorn, L. Böger, R. Adelung and K. Schulte, Direction sensitive bending sensors based on multi-wall carbon nanotube/epoxy nanocomposites, *Nanotechnology* **19**, 475503 (2008).
21. N. Hu, Y. Karube, C. Yan, Z. Masuda and H. Fukunaga, Tunneling effect in a polymer/carbon of nanotube nanocomposite strain sensor, *Acta Mater*. **56**, 2929–2936 (2008).
22. M. Knite, V. Tupureina, A. Fuith, J. Zavickis and V. Teteris, Polyisoprene — multi-wall carbon nanotube composites for sensing strain, *Mater. Sci. Engng C* **27**, 1125–1128 (2007).
23. L Bokabza and C. Belin, Effect of strain on the properties of a styrene–butadiene rubber filled with multiwall carbon nanotubes, *J. Appl. Polym. Sci*. **105**, 2054–2061 (2007).
24. M. Taya, W. J. Kim and K. Ono, Piezoresistivity of a short fiber/elastomer matrix composite, *Mech. Mater*. **28**, 53–59 (1998).
25. S. Iijima, Helical microtubules of graphitic carbon, *Nature* **354**, 56–58 (1991).
26. A. Oberlin, M. Endo and T. Koyama, Filamentous growth of carbon through benzene decomposition, *J. Cryst. Growth* **32**, 335–349 (1976).
27. S. R. Broadbent and J. M. Hammersler, Percolation processes I. Crystals and mazes, *Proc. Cambridge Philos. Soc*. **53**, 629–641 (1957).
28. S. Kirkpatrick, Percolation and conduction, *Rev. Mod. Phys*. **45**, 574–588 (1973).
29. G. E. Pike and C. H. Seager, Percolation and conductivity: a computer study. I, *Phys. Rev. B* **10**, 1421–1434 (1974).
30. N. Ueda and M. Taya, Prediction of the electrical conductivity of two-dimensionally misoriented short fiber composites by a percolation model, *J. Appl. Phys*. **60**, 459–461 (1986).

31. M. Taya and N. Ueda, Prediction of the on-plane electrical conductivity of a misoriented short fiber composite: fiber percolation model *versus* effective medium theory, *Trans. ASME, J. Eng. Mater. Technol*. **109**, 252–256 (1987).
32. A. Allaoui, S. V. Hoa and M. D. Pugh, The electronic transport properties and microstructure of carbon nanofiber/epoxy composites, *Compos. Sci. Technol*. **68**, 410–416 (2008).
33. J. G. Simmons, Generalized formula for the electric tunnel effect between similar electrodes separated by a thin insulating film, *J. Appl. Phys*. **34**, 1793–1803 (1963).
34. H. Ago, T. Kugler, F. Cacialli, W. R. Salaneck, M. S. P. Shaffer, A. H. Windle and R. H. Friend, Work functions and surface functional groups of multiwall carbon nanotubes, *J. Phys. Chem. B* **103**, 8116–8121 (1999).